Pergamon

Tetrahedron 56 (2000) 753–761

TETRAHEDRON

Salts of *N*,*N*′-Oxalylbis(phenylglycine)s and 1-Phenylethylamines: Structural Variation of Layered Materials Induced by Stereochemistry

Motohiro Akazome,[a] Toshiaki Takahashi,[b] Naoyuki Ito,[a] Noriyuki Baba[a] and Katsuyuki Ogura[a,*]

[a]*Department of Materials Technology, Faculty of Engineering, Chiba University, 1-33 Yayoicho, Inageku, Chiba 263-8522, Japan*
[b]*Graduate School of Science and Technology, Chiba University, 1-33 Yayoicho, Inageku, Chiba 263-8522, Japan*

Received 2 November 1999; accepted 8 December 1999

Abstract—Salts between (*R*,*R*)- or *meso*-*N*,*N*′-oxalylbis(phenylglycine) **1** and (*R*)-, (*S*)-, or (±)-1-phenylethylamine **2** construct three different layer structures depending on their stereochemistry. By X-ray crystallography, it is elucidated that the formation of a hydrogen bonding network between the amino and carboxyl groups and the planarity of the oxalyl functionality are important to construct the sheet structure. The salt of (*R*,*R*)-**1** and **2** forms a bilayer or puckered structure, whereas the salt of *meso*-**1** and **2** constructs a monolayer structure.

Introduction

In crystal engineering, two-dimensional inorganic networks have been extensively studied from the standpoint of solid-state supramolecular chemistry.[1] Recently, two-dimensional organic molecules were designed so as to control their aggregation and, as a result, construct layer structures.[2] Zaworotko et al. reported supramolecular synthesis of organic laminates using affinity to aromatic guests.[3] It was also reported by Ward et al. that guanidium alkane- and arenesulfonates construct a bilayer or monolayer structure depending on the size of alkyl and aryl groups.[4] Napthalenedicarboxamides were shown by Lewis et al. to form a monolayer or bilayer structure according to the position of their substituents.[5] Furthermore, Aarkeröy et al. reported the hydrogen-bonding layers of hydrogen malate anions as well as the influence of their counter ions on the geometry and crystal packing.[6]

Our attention was focused on a salt of an optically active amine and an *N*,*N*′-oxalylbis(α-amino acid) because the latter is well-known to construct a two-dimensional sheet structure, in which the central oxalamide unit adopts a planar and *trans* configuration.[7,8] Here we report that the salt of *N*,*N*′-oxalylbis(phenylglycine) **1** and 1-phenylethylamine **2** forms a monolayer or bilayer structure according to the stereochemistry of each component, as summarized in Chart 1: A bilayer structure was given by the salt of (*R*,*R*)-**1** and (±)- or (*R*)-**2**, while the salt of *meso*-**1** and (±)-**2** formed a monolayer structure.[9] Furthermore, the salt of (*R*,*R*)-**1** and (*S*)-**2** gave rise to the formation of another layer structure which is called "a puckered layer". These facts are in sharp contrast with the case of organic salts between 1-phenylethylamine and such chiral carboxylic acids as cholic acids,[10] phenylpropionic acid[11] and mandelic acids,[12] which construct helical columnar structures.

Results and Discussion

Synthesis of (*R*,*R*)- or *meso*-1 and these salts

According to Scheme 1, (*R*,*R*)-**1** was easily prepared by the coupling of oxalyl chloride and (*R*)-phenylglycine benzyl ester followed by hydrogenolysis to remove the protecting benzyl groups. Some difficulties were encountered in a similar synthesis of *meso*-**1** starting from *racemic* phenylglycine benzyl ester to obtain the product in a pure state. Hence, oxalyl chloride reacted with a 1:1 mixture of (*R*)-phenylglycine benzyl ester and (*S*)-phenylglycine methyl ester to afford a statistic mixture (1:2:1) of oxalyl amides. After the separation of their differentially protected products using column chromatography, stepwise deprotection of the benzyl and the methyl groups was performed by hydrogenolysis and acid-catalyzed hydrolysis, respectively, to afford *meso*-**1** in a pure form.

These (*R*,*R*)- or *meso*-**1** reacted with (*R*)-, (*S*)-, or (±)-**2** in methanol to form a homogenous solution of the corresponding salt. Slow evaporation of the methanol deposited the 1:2 salts of **1** and **2** in a crystalline state. In order to prepare the

Keywords: ammonium salts; amino acids; stereochemistry; X-ray crystal structure.
* Corresponding author. Tel.: +81-43-290-3388; fax: +81-43-290-3402; e-mail: katsu@planet.tc.chiba-u.ac.jp

0040–4020/00/$ - see front matter
PII: S0040-4020(99)01059-5

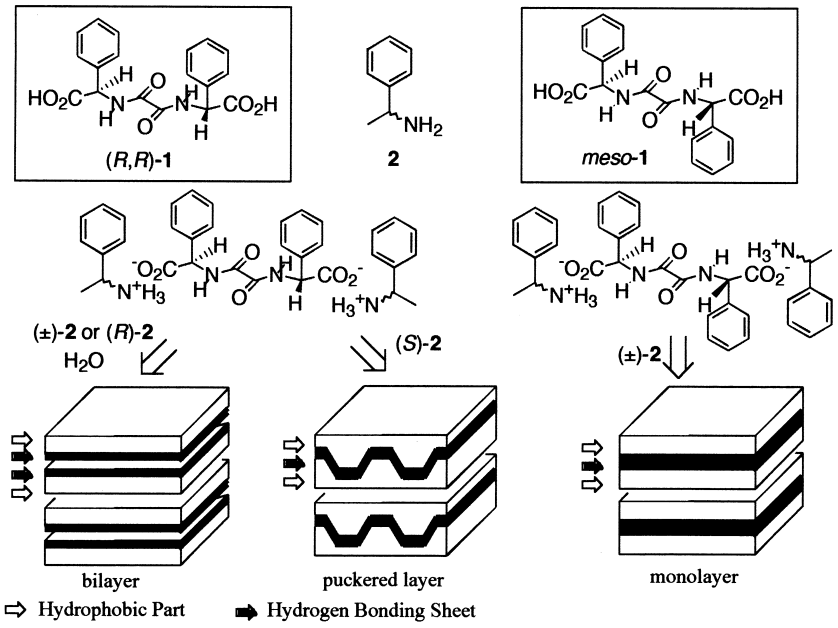

Chart 1.

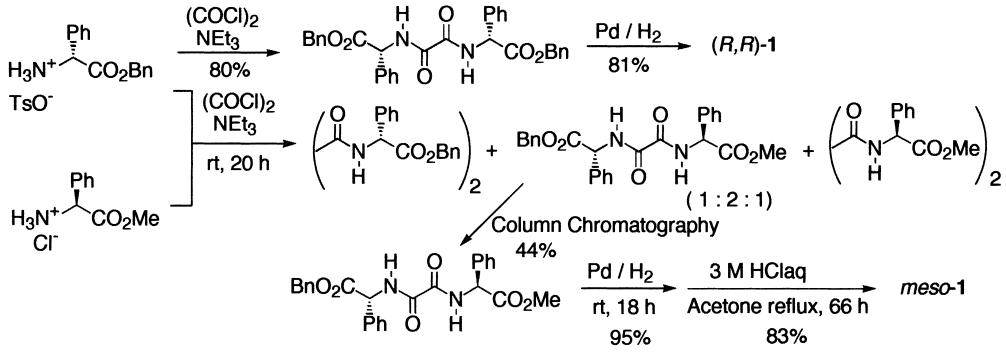

Scheme 1.

Table 1. Crystal data and data collection parameters

Data	(*R*,*R*)-**1**·(±)-**2**·H_2O	(*R*,*R*)-**1**·(*R*)-**2**·H_2O	(*R*,*R*)-**1**·(*S*)-**2**	*meso*-**1**·(±)-**2**
Formula	$C_{34}H_{40}N_4O_7$	$C_{34}H_{40}N_4O_7$	$C_{34}H_{38}N_4O_6$	$C_{17}H_{19}N_2O_3$
Formula weight	616.71	616.71	598.70	299.35
Crystal system	Monoclinic	Monoclinic	Monoclinic	Triclinic
Space group	$P2_1$	$P2_1$	$P2_1$	$P\bar{1}$
T (K)	298	298	173	173
a (Å)	14.605(3)	14.747(3)	19.946(6)	15.917(5)
b (Å)	10.034(3)	9.952(3)	5.557(3)	10.345(4)
c (Å)	12.129(3)	12.251(3)	14.580(5)	5.072(2)
α (°)				86.13(3)
β (°)	104.44(2)	106.27(2)	108.97(3)	94.34(3)
γ (°)				74.76(3)
V (Å^3)	1721.5(8)	1725.9(6)	1528(1)	800.2(4)
Z	2	2	2	2
D_{calcd}	1.19	1.186	1.301	1.242
Radiation used	Cu-$K\alpha$	Cu-$K\alpha$	Cu-$K\alpha$	Cu-$K\alpha$
μ (mm^{-1})	0.610	0.684	0.7325	0.6995
Measured reflections	3468	3470	3219	3074
Observed reflections	3040	2152	2786	1897
Criteria of I	3	3	3	1.5
R	0.0446	0.040	0.060	0.074
wR	0.0519	0.043	0.062	0.066
Residual electron density	0.15, −0.22	0.20, −0.18	0.83, −0.54	0.22, −0.25

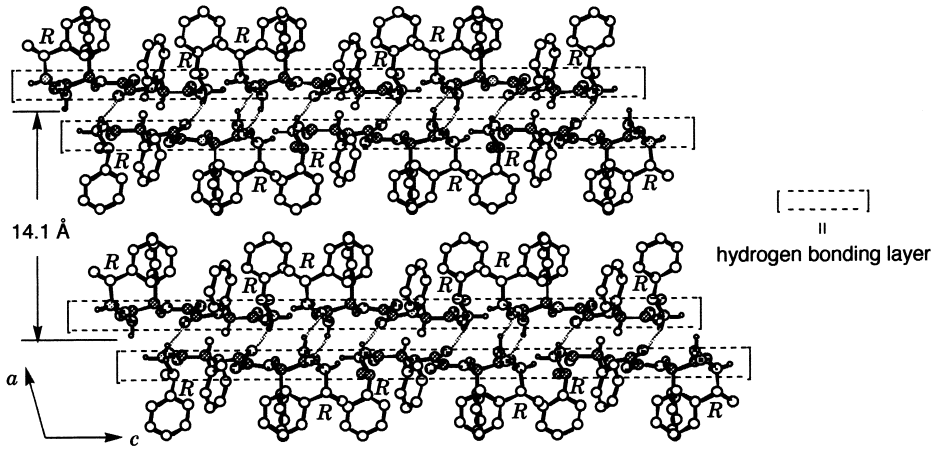

Figure 1. A bilayer structure of (*R*,*R*)-**1**·(*R*)-**2**·H_2O (*a*–*c* plane). Alkyl and phenyl groups are colored white.

corresponding anhydrous salts, dry methanol was used as a solvent and the crystallization process was performed in a desiccator.

X-Ray diffraction analysis for salts of 1 and 2

Among the possible combinations of **1** [(*R*,*R*)- or *meso*-**1**] and **2** [(*R*)-, (*S*)-, or (±)-**2**], four kinds of salts, i.e. (*R*,*R*)-**1**·(±)-**2**·H_2O,[9] (*R*,*R*)-**1**·(*R*)-**2**·H_2O, (*R*,*R*)-**1**·(*S*)-**2**, and *meso*-**1**·(±)-**2** were obtained as single crystals. The data of their single-crystal X-ray analyses are summarized in Table 1.

In addition to the single-crystal analyses, X-ray powder diffraction (XRPD) analyses gave us important information about their layered structures. In all these salts, a strong diffraction peak was observed at a lower range of 2Θ angle. This peak corresponds to a layer distance (vide infra).

The salts of (*R*,*R*)-**1** and (±)- or (*R*)-**2** included water, but other salts were obtained as anhydrous salts even under wet conditions. By carefully keeping anhydrous conditions, anhydrous salts of (*R*,*R*)-**1**·(±)-**2** and (*R*,*R*)-**1**·(*R*)-**2** could be prepared. In XRPD patterns of these anhydrous salts, no characteristic strong peak was observed (see Fig. 10).

Bilayer structure: the salts of (*R*,*R*)-1 and (±)- or (*R*)-2

The crystal of (*R*,*R*)-**1**·(*R*)-**2**·H_2O formed a bilayer structure (Fig. 1), which is an isostructure of (*R*,*R*)-**1**·(±)-**2**·H_2O (Fig. 3). In the bilayer structure, the half-layer consists of a hydrophilic hydrogen bonding sheet and a hydrophobic part containing phenyl and alkyl groups. Two half-layers are paired via hydrogen bonding interaction between their hydrophilic layers. The XRPD pattern showed a strong peak at 14.1 Å, which corresponded to the layer distance between the (100) planes in Fig. 1.

As seen in Fig. 2a, the hydrophilic hydrogen bonding sheet shows that the conformation of an oxalyl linkage is a somewhat distorted transoid[13] (the torsion angle of O^2–C^{14}–C^{17}–O^8=168.9°). The salt formation between the amino and carboxyl groups constructed a 12-membered ring;[14] bond distances are 2.80 Å for $N^{10}\cdots O^5$, 2.73 Å for $N^{10}\cdots O^4$, 2.73 Å for $N^6\cdots O^1$, and 2.90 Å for $N^6\cdots O^3$. By the aid of water molecules, which bind simultaneously to the amino and carboxyl groups ($N^6\cdots O^9$, 2.89 and $O^{*5}\cdots O^9$, 2.83 Å), the one-dimensional backbones of the salts combine to form a two-dimensional sheet structure.

Two hydrophilic layers are combined by two hydrogen

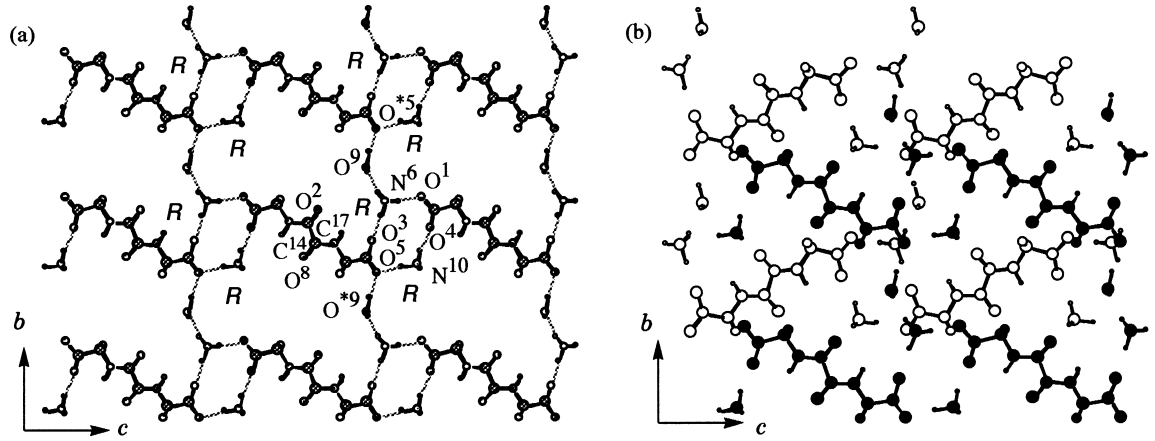

Figure 2. (a) The hydrogen bonding layer of the salt of (*R*,*R*)-**1**·(*R*)-**2**·H_2O (*b*–*c* plane). (b) The offset between two layers (*b*–*c* plane). Alkyl and phenyl groups are omitted.

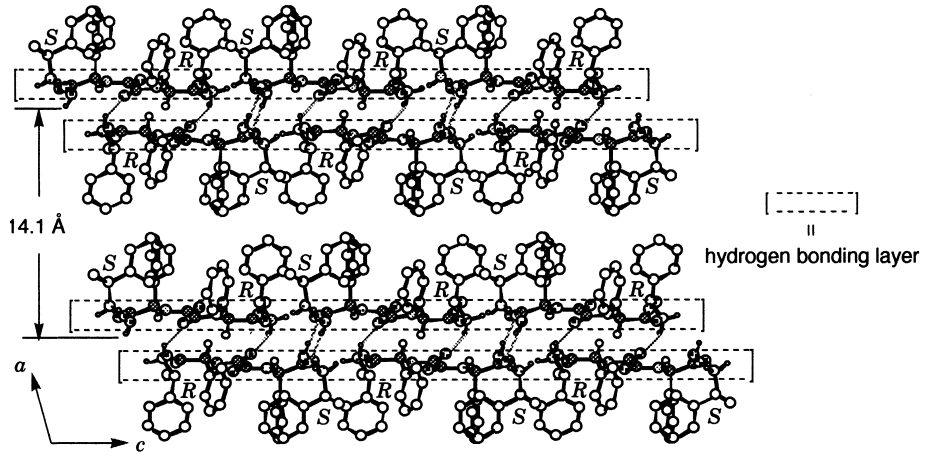

Figure 3. A bilayer structure of (*R*,*R*)-**1**·(±)-**2**·H_2O (*a*–*c* plane). Alkyl and phenyl groups are colored white.

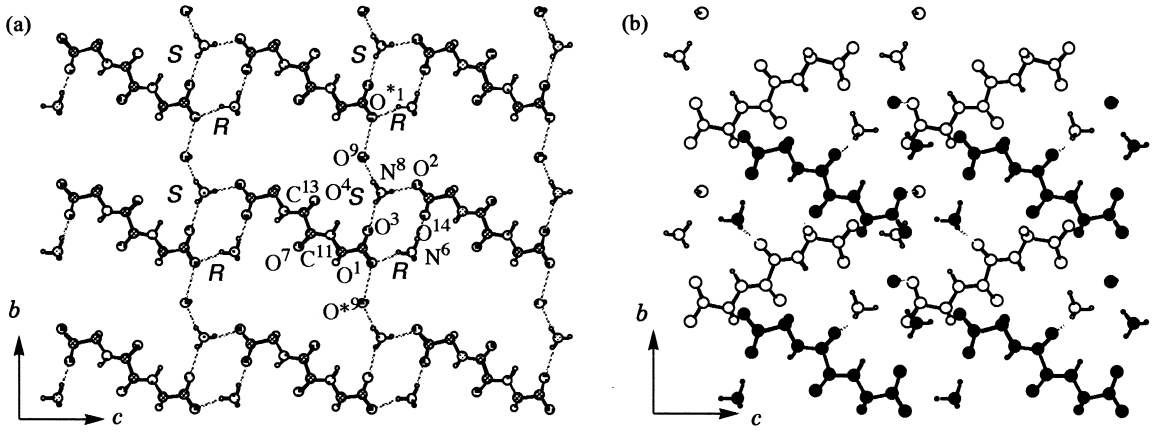

Figure 4. (a) The hydrogen bonding layer of the salt of (*R*,*R*)-**1**·(±)-**2**·H_2O (*b*–*c* plane). (b) The offset between two layers (*b*–*c* plane). Alkyl and phenyl groups are omitted.

bonds (Fig. 1); one hydrogen bond is between the water and a carboxylate ($O^9\cdots O^3$, 2.76 Å) and the other is between a nitrogen of ammonium and an oxygen of the oxalyl group ($N^{10}\cdots O^2$, 2.88 Å). The two hydrophilic layers stack in a face-to-face manner to become the bilayer structure (Fig. 2b).

The crystal of (*R*,*R*)-**1**·(±)-**2**·H_2O[9] also has a bilayer structure, which consists of (*R*,*R*)-**1**, (*R*)-**2** and (*S*)-**2**, and water (Fig. 3). The XRPD pattern shows a strong peak at 14.1 Å corresponding to the layer distance between the (100) planes. The hydrogen bonding sheet (Fig. 4) of (*R*,*R*)-**1**·(±)-**2**·H_2O is very similar to that of (*R*,*R*)-**1**·(*R*)-**2**·H_2O.

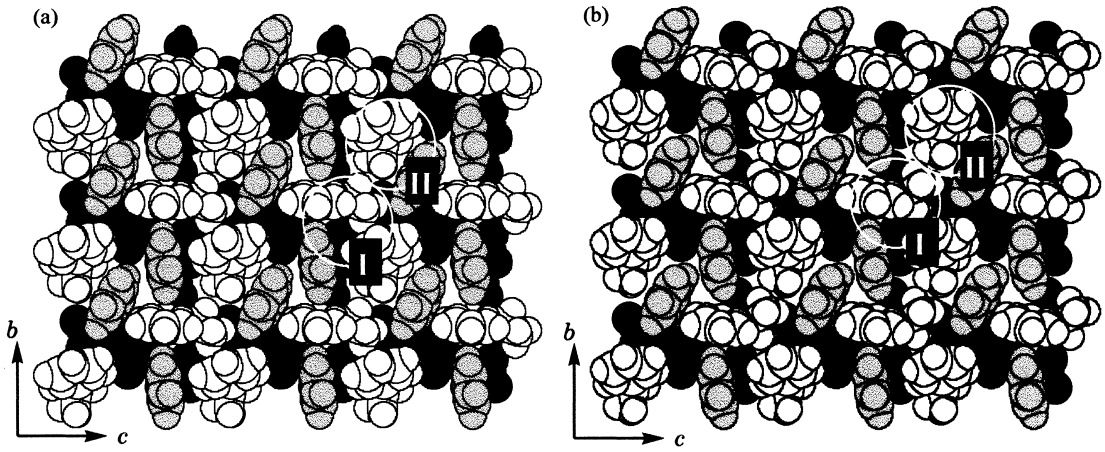

Figure 5. Similarity of crystal packing. (a) (*R*,*R*)-**1**·(*R*)-**2**·H_2O, (*R*)-**2** in Regions I and II. (b) (*R*,*R*)-**1**·(±)-**2**·H_2O, (*S*)-**2** in Region I and (*R*)-**2** in Region II.

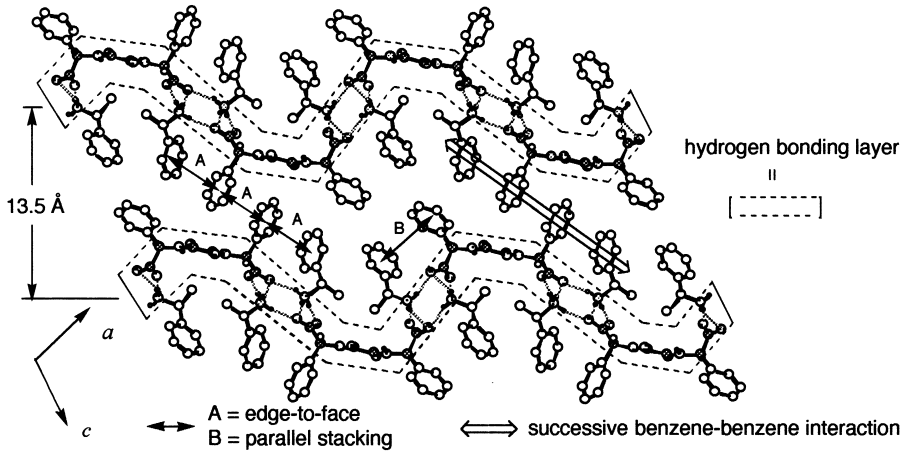

Figure 6. Puckered layer of (*R*,*R*)-**1**·(*S*)-**2** (*a*–*c* plane). Alkyl and phenyl groups are colored white.

The hydrophobic parts of these two salts are shown in a space filling model (Fig. 5). Region I is tolerant for the stereochemistry of **2**, but region II permitted only the *R* form of **2**. Therefore, it is assumed that, if (*S*)-**2** is enclosed instead of (*R*)-**2**, region II has to change its shape. Indeed, the steric repulsion of region II compelled the structure of (*R*,*R*)-**1**·(*S*)-**2** to adopt a puckered layer (vide infra).

If (*R*)-**2** molecules are included between such puckered layers, they would undergo steric repulsion and, as a result, the bilayer structure was constructed by the incorporation of water.

Puckered layer structure: a salt of (*R*,*R*)-1 and (*S*)-2

Even when crystallization was performed in the presence of water, the anhydrous salt of (*R*,*R*)-**1** and (*S*)-**2** was obtained. Fig. 6 shows that the crystal structure has a puckered sheet of (*R*,*R*)-**1**·(*S*)-**2**. One hydrophobic layer of (*R*,*R*)-**1**·(*S*)-**2** has two different modes of benzene–benzene packing, one is "edge-to-face (tilted T)" and the other is "parallel stacking (parallel stacked and displaced)" (A and B in Fig. 6).[15] It is also shown that a strong peak (13.5 Å) of the XRPD pattern corresponds to the layer distance between the (101) planes. Between the puckered sheets, an edge-to-face interaction of phenyl groups is also observed, where successive edge-to-face of four benzene rings realize the puckered layer. Since the conformation of an oxalyl linkage is a somewhat distorted transoid[13] (the torsion angle of O^4–C^{14}–C^{12}–O^5=176.2°), two phenyl groups of (*R*,*R*)-**1** stand on one side of the backbone of (*R*,*R*)-**1**.

In one monolayer structure (Fig. 7), the salt formation between the amino and carboxyl groups constructed two different 10-membered rings; one has $N^{42}\cdots O^{2}$ (2.70 Å), $N^{42}\cdots O^{1}$ (2.79 Å), and $N^{42}\cdots O^{*1}$ (2.80 Å), the other has $N^{52}\cdots O^{40}$ (2.69 Å), $N^{52}\cdots O^{41}$ (2.74 Å), and $N^{52}\cdots O^{*41}$ (3.06 Å). These 10-membered rings are often observed in the helical hydrogen-bond columns (2_1-column) of amine salts of carboxylic acids.[12a,14a]

Monolayer structure: a salt of *meso*-1 and (±)-2

Crystals of *meso*-**1**·(±)-**2** did not include any water molecule. The crystal structure of this salt has a center of symmetry and shows a monolayer structure (Fig. 8). In addition to salt formation, benzene–benzene interactions were also observed, where the (*R*)- and (*S*)-phenylglycine moieties of *meso*-**1** interacted with the phenyl group of (*R*)- and (*S*)-**2**, respectively. The XRPD pattern showed a strong peak at 15.5 Å, which corresponded to the layer distance between the (100) planes.

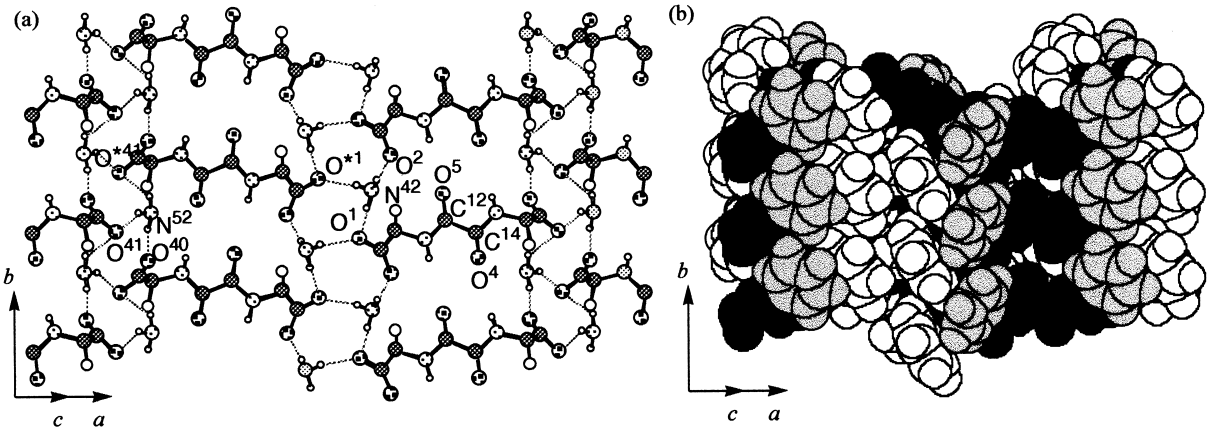

Figure 7. (a) Hydrogen bonds of a puckered layer of (*R*,*R*)-**1**·(*S*)-**2**. (b) CPK model. Alkyl and phenyl groups of (*R*,*R*)-**1** and (*S*)-**2** or coloured white and gray, respectively.

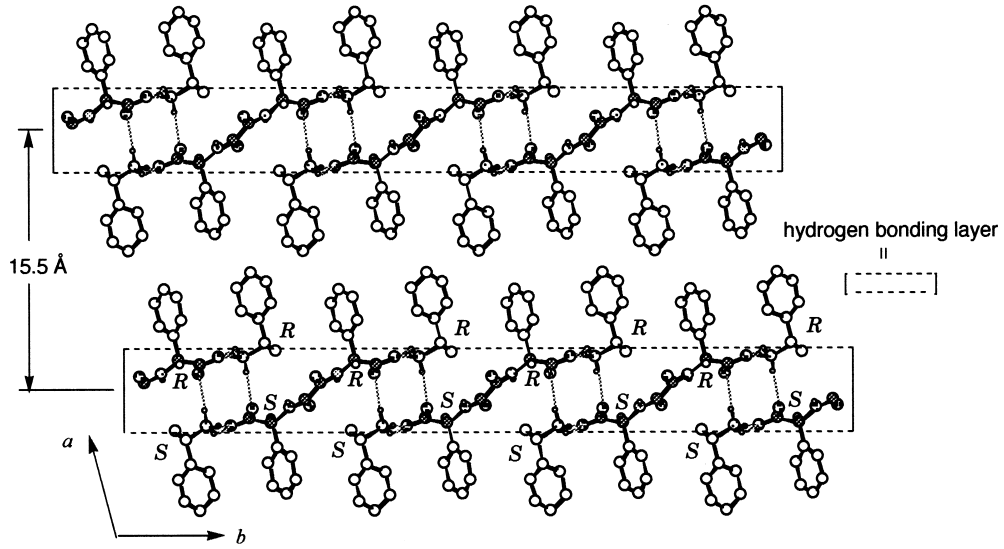

Figure 8. A monolyer structure of *meso*-1·(±)-**2** (*a*–*b* plane). Alkyl and phenyl groups are colored white.

Since the conformation of an oxalyl linkage is perfectly transoid[13] (the torsion angle of O^4–C^6–C^{*6}–O^{*4}=180.0°) and fixes the conformation of *meso*-**1** to be flat, two phenyl groups of *meso*-**1** stand above and below the backbone sheet.

Fig. 9a shows the salt formation and hydrogen bonding network in the monolayer structure: $N^5\cdots O^2$ (2.73 Å), $N^5\cdots O^3$ (2.78 Å), $N^5\cdots O^{*3}$(2.94 Å), and $N^5\cdots O^{*2}$ (2.99 Å). Phenyl groups of *meso*-**1**·(±)-**2** construct a herringbone motif via the edge-to-face interactions (Fig. 9b).

Another salt, *meso*-**1**·(*R*)-**2**, is also shown to include no water molecule. Since its XRPD pattern and IR spectrum are very similar to those of *meso*-**1**·(±)-**2**, the salt of *meso*-**1**·(*R*)-**2** can be assumed to be a monolayer structure.

Hydration of anhydrous (*R*,*R*)-1·2 salts: X-ray powder diffraction analysis for these layers

As mentioned above, anhydrous salts [(*R*,*R*)-**1**·(±)-**2** and (*R*,*R*)-**1**·(*R*)-**2**] were prepared by crystallization from dry methanol. Their compositions were also confirmed by elemental analysis.

Interestingly, after anhydrous (*R*,*R*)-**1**·(±)-**2** and (*R*,*R*)-**1**·(*R*)-**2** were exposed to water vapor for a few weeks, hydration of these anhydrous salts occurred. The XRPD pattern of these hydrated solids became similar to those of (*R*,*R*)-**1**·(±)-**2**·H_2O and (*R*,*R*)-**1**·(*R*)-**2**·H_2O, respectively (Fig. 10). These results supported that the water molecules play an important role in constructing the hydrogen bonding network in the bilayer structures of (*R*,*R*)-**1**·(±)-**2**·H_2O and (*R*,*R*)-**1**·(*R*)-**2**·H_2O.

On the other hand, the water molecules were hardly removed from both hydrated (*R*,*R*)-**1**·(*R*)-**2** and (*R*,*R*)-**1**·(±)-**2** at room temperature. When hydrated salts were heated, the dehydration occurred above 150°C to decompose both the salts.

Conclusion

In this paper, we demonstrated that the oxalyl functionality, which combined two phenylglycine parts, makes the backbone of *N*,*N*′-oxalylbis(phenylglycine) fairly flat, and the salt formation between **1** and **2** constructs a sheet structure with the aid of hydrogen bonds.

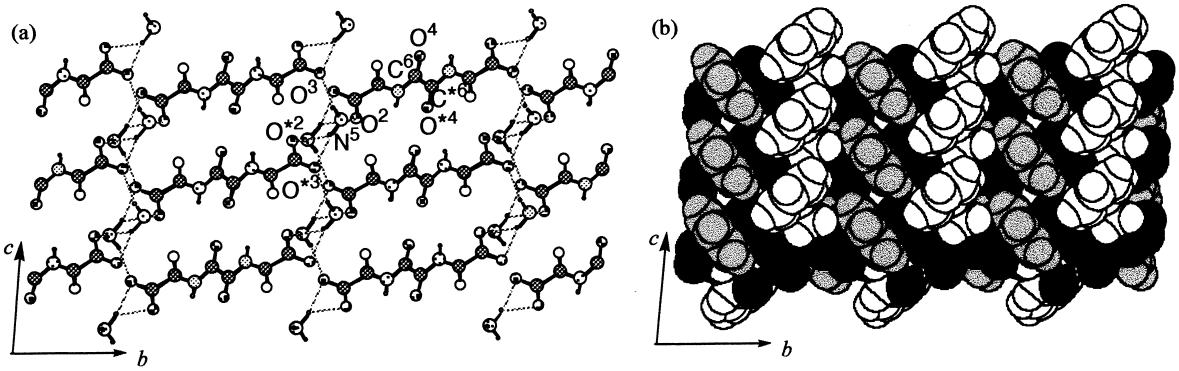

Figure 9. (a) Hydrogen bonds of a monolayer structure of *meso*-**1**·(±)-**2**. (b) CPK model. Alkyl and phenyl groups of *meso*-**1** and (±)-**2** are colored white and gray, respectively.

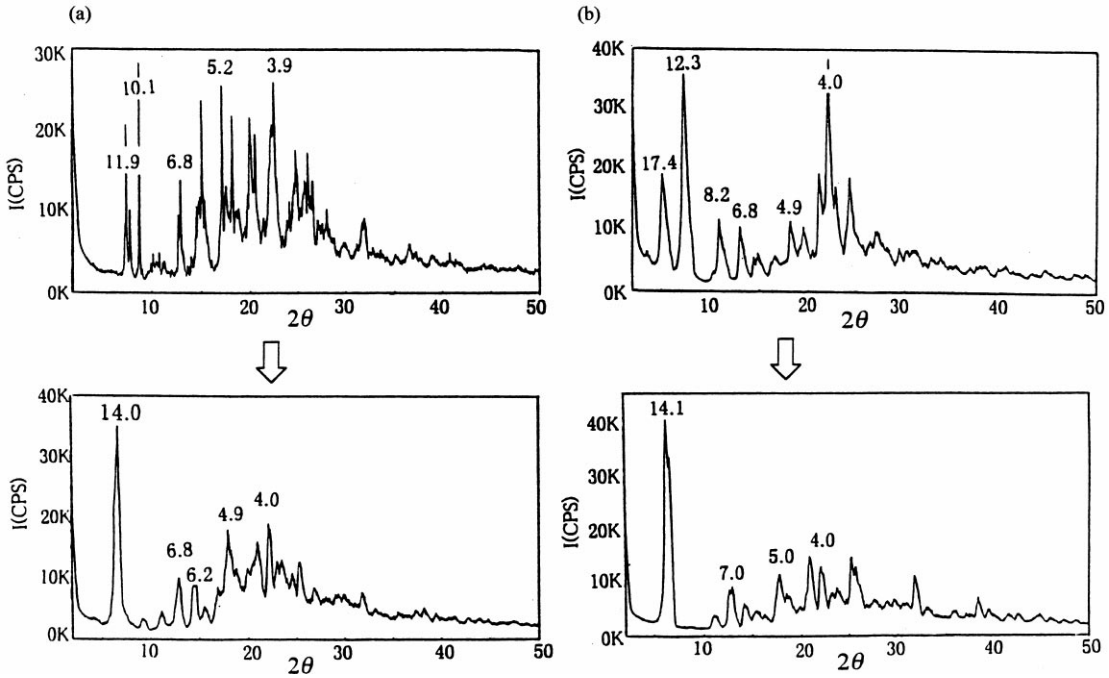

Figure 10. Change of the powder X-ray diffraction by hydration of the salts: (a) (*R*,*R*)-**1**·(*R*)-**2**; (b) (*R*,*R*)-**1**·(±)-**2**. Selected distances (Å) corresponding to 2θ values are shown on each peak.

Three different layer structures formed according to the combination of the stereochemical isomers of **1** and **2**. The salt of (*R*,*R*)-**1** and (±)- or (*R*)-**2** included water molecules, which construct a bilayer structure. These crystal structures of the hydrated salts were isostructural. Under anhydrous conditions, anhydrous (*R*,*R*)-**1**·(±)-**2** and (*R*,*R*)-**1**·(*R*)-**2** were obtained. On the other hand, the salt of (*R*,*R*)-**1** and (*S*)-**2** showed quite a different structure, a puckered layer. The salt of *meso*-**1** and (±)-**2** has a monolayer structure. Thus, it was found that the structural variation of these layered materials depends on the stereochemistry of **1** and **2**. These results suggest that the stereochemistry of amino acids takes an important role in crystal engineering. In symmetric molecules bearing two chiral centers, D,L- and *meso*-forms are possible. Although Aakeröy et al. have prepared salts between L- or *meso*-tartaric acid and (*S*)-**2**, their crystal structures showed only a monolayer structure.[16] Our design of phenylglycine derivatives based on the stereochemistry will make it possible to adopt various two-dimensional crystal arrangements.

Experimental

General

^{1}H NMR spectra were recorded on a Varian Gemini 2000 spectrometer. The infrared spectra were recorded on a JASCO Herschel FT/IR-350. The melting points were measured on a hot-stage microscope apparatus (Yanagimoto) and are uncorrected. (*R*)-Phenylglycine (99% ee), (*S*)-phenylglycine (99% ee), *racemic* 1-phenylethylamine, (*R*)-1-phenylethylamine (99% ee) and (*S*)-1-phenylethylamine (99% ee) were purchased from Tokyo Kasei Kogyo.

Powder X-ray diffraction

All XRPD analyses were taken on a MAC Science MXP powder diffractometer using graphite-monochromated Cu*K*α radiation (40 kV, 300 mA). The spectra were measured between 2 and 50° in the 2θ/θ-scan mode with steps of 0.01° in 2θ and 4°/min.

X-Ray crystallography

Data collection was performed on a Mac Science MXC18 four-circle diffractometer with monochromated Cu*K*α (λ=1.54178 Å) radiation using the 2θ–ω scan technique, and the X-ray intensities were measured up to 2θ=140°. Three standard reflections were monitored every 100 reflections; there were no significant variations in intensities. The structures were solved and refined on direct methods (SIR 92[17] on a computer program package; CRYSTAN-GM ver. 6.2.1 or maXus ver. 1.1 from MAC Science Co. Ltd.) Further detail data have been deposited with the Cambridge Crystallographic Data Centre.[18]

Synthesis of (*R*,*R*)-*N*,*N*′-oxalylbis(phenylglycine) [(*R*,*R*)-1]

Oxalyl chloride (3.02 mL, 34.6 mmol) in dry diethyl ether (80 mL) was added dropwise into a mixture of (*R*)-phenylglycine benzyl ester *p*-tolenesulfonate[19] (29.7 g, 71.8 mmol), triethylamine (19.5 mL, 140 mmol), and dry diethyl ether (250 mL) over 40 min at 0°C, and stirred for 18 h at ambient temperature. After evaporation of the solvent, ethyl acetate (400 mL) was added and insoluble salts were filtered. Organic residue was washed by 0.6 M aqueous HCl (100 mL×3), 5% $NaHCO_3$ (200 mL×3), and water (100 mL), dried over $MgSO_4$ and evaporated. The

residue was recrystallized from hexane/ethyl acetate to give *O*,*O*′-dibenzyl *N*,*N*′-oxalylbis(phenylglycine) (15.0 g, 27.9 mmol, 80%) as colorless crystals: mp 157–158°C; $[\alpha]_D^{25}=-123.5$ (c=1.00, $CHCl_3$); ^{1}H NMR(300 MHz: $CDCl_3$) δ 5.13 (d, J=12.4 Hz, 2H), 5.22 (d, J=12.4 Hz, 2H), 5.55 (d, J=7.6 Hz, 2H), 7.16–7.32 (m, 20H), 8.25 (d, J=7.6 Hz, 2H); IR (KBr): 3300, 1740, 1660, 1538, 1506, 1454, 1314, 1172, 728, 696 cm^{-1}. *O*,*O*′-Dibenzyl *N*,*N*′-oxalylbis(phenylglycine) (10.5 g, 19.5 mmol) was dissolved in MeOH (300 mL), and treated with hydrogen in the presence of palladium black (prepared from $PdCl_2$ 902 mg) as a catalyst for 18 h. The catalyst was removed by filtration, and concentration of the filtrate gave a solid. Crystallization of the solid from methanol afforded (*R*,*R*)-**1** (5.67 g, 15.9 mmol, 81%) as a colorless powder: mp 225°C dec.; $[\alpha]_D^{25}=-231.5$ (c=1.01, methanol); ^{1}H NMR (300 MHz: d^6-DMSO) δ 5.42 (d, J=7.7 Hz, 2H), 7.30–7.42 (m, 10H), 9.02 (d, J=7.7 Hz, 2H); IR (KBr): 3300, 3140, 2930, 1718, 1660, 1506, 1416, 1224, 1088, 1069, 726, 696 cm^{-1}. Anal. Calcd for $C_{18}H_{16}N_2O_6$: C, 60.67; H, 4.53; N, 7.86. Found: C, 60.51; H, 4.44; N, 7.77.

Synthesis of *meso*-*N*,*N*′-oxalylbis(phenylglycine) [*meso*-1]

Oxalyl chloride (0.87 mL, 10.0 mmol) was added dropwise into a mixture of (*R*)-phenylglycine benzyl ester *p*-toluenesulfonate[19] (4.14 g, 10.0 mmol), (*S*)-phenylglycine methyl ester hydrochloride[20] (2.02 g, 10.0 mmol), triethylamine (5.60 mL, 40.0 mmol), and dry THF (100 mL) over 30 min at 0°C, and stirred for 24 h at ambient temperature. After evaporation of the solvent, ethyl acetate (300 mL) was added and insoluble salts were filtered. Organic residue was washed by 10% aqueous citric acid (100 mL×3), brine (100 mL×3), and saturated $NaHCO_3$ (100 mL×3), dried over $MgSO_4$, and evaporated. The crude products were separated by careful silica gel column chromatography (eluent, hexane/AcOEt=2:1) to give *O*-benzyl *O*′-methyl *meso*-**1** (1.81 g, 2.71 mmol, 44 %) as a colorless powder: mp 170.8°C dec.; ^{1}H NMR (300 MHz: $CDCl_3$) δ 3.73 (s, 3H), 5.12 (d, J=14.0 Hz, 1H), 5.20 (d, J=14.0 Hz, 1H), 5.51(d, J=7.6 Hz, 1H), 5.55 (d, J=7.6 Hz, 1H), 7.30–7.42 (m, 10H), 8.22 (d, J=7.6 Hz, 1H), 8.24 (d, J=7.6 Hz, 1H); IR (KBr): 3316, 2362, 2344, 1736, 1662, 1508, 1173, 696 cm^{-1}. Anal. Calcd for $C_{24}H_{24}N_2O_6$: C, 66.96; H, 5.62; N. 6.51. Found: C, 66.85; H, 5.74; N. 6.40. *O*-Benzyl *O*′-methyl *meso*-**1** (223 mg, 0.48 mmol) was dissolved in MeOH (80 mL), and treated with hydrogen in the presence of palladium black (prepared from $PdCl_2$ 92 mg) as a catalyst for 18 h. The catalyst was removed by filtration, and concentration of the filtrate gave *O*-methyl *meso*-**1** (173 mg, 0.46 mmol, 95%) as a colorless powder. To *O*-methyl *meso*-**1** in acetone (60 mL), 3 M aqueous HCl (20 mL) was added and stirred under reflux conditions for 66 h. The concentration of the reaction mixture gave a solid and crystallization from methanol afford *meso*-**1** (136 mg, 0.38 mmol, 83%) as a white powder: mp 235°C dec.; ^{1}H NMR (300 MHz: d^4-MeOH) δ 5.46 (s, 2H), 7.31–7.48 (m, 10H); IR (KBr): 3286, 3934, 2921, 1719, 1664, 1520, 1420, 1220, 1093, 1068, 934, 723, 695 cm^{-1}. Anal. Calcd for $C_{18}H_{16}N_2O_6$: C, 60.67; H, 4.53; N. 7.86. Found: C, 60.50; H, 4.47; N. 7.69.

General synthesis of salts between 1 and 2

To prepare salts of **1** (34 mg, 0.11 mmol) and **2** (37 mg, 0.33 mmol), both of them were dissolved in water (2.0 mL) or dry methanol (2.0 mL) in a vial. The vial was kept for a few days. For anhydrous salts, the vial was stored over P_2O_5 in a desiccator under anhydrous conditions.

*(R,R)-**1**·(±)-**2**·H$_2$O:* colorless plate crystals: mp 161°C dec.; ^{1}H NMR (300 MHz: D_2O) δ 1.63 (d, J=7.0 Hz, 6H), 4.51 (q, J=7.0 Hz, 2H), 5.15 (s, 2H), 7.34–7.51 (m, 20H). IR (KBr): 3384, 3345, 3168, 3060, 3023, 2945, 2100, 1671, 1577, 1476, 1377, 1236, 1172, 1066, 968, 699 cm^{-1}; Powder X-ray Analysis (I/I_0) 14.04 Å (1.00), 7.04 Å (0.20), 4.70 Å (0.02), 4.25 Å (0.03), 3.53 Å (0.13), 2.82 Å (0.06). Anal. Calcd for $C_{34}H_{40}N_4O_7$: C, 66,21; H, 6.54; N, 9.08. Found: C, 66.50; H, 6.49; N, 9.28.

*Anhydrous (R,R)-**1**·(±)-**2**:* colorless plate crystals: mp 152.5°C dec.; ^{1}H NMR (300 MHz: D_2O) δ 1.61 (d, J=6.9 Hz, 6H), 4.48 (q, J=6.9 Hz, 2H), 5.15 (s, 2H), 7.26–7.53 (m, 20H); IR (KBr): 3385, 3070, 3038, 2980, 2930, 2180, 1671, 1577, 1491, 1389, 1236, 1190, 1091, 1068, 1030, 700 cm^{-1}; Powder X-ray Analysis (I/I_0) 17.42 Å (0.44), 12.30 Å (1.00), 8.17 Å (0.28), 6.80 Å (0.26), 4.90 Å (0.20), 4.54 Å (0.13), 4.20 Å (0.38), 4.02 Å (0.89), 3.87 Å (0.18), 3.65 Å (0.36). Anal. Calcd for $C_{34}H_{38}N_4O_6$: C, 68.21; H, 6.40; N, 9.36. Found: C, 68.17; H, 6.41; N, 9.33.

*(R,R)-**1**·(R)-**2**·H$_2$O:* colorless plate crystals: mp 174°C dec.; ^{1}H NMR (300 MHz: d^4-CD_3OD) δ 1.62 (d, J=6.9 Hz, 6H), 4.48 (q, J=6.9 Hz, 2H), 5.14 (s, 2H), 7.36–7.45 (m, 20H); IR (KBr): 3386, 3343, 3068, 3038, 2960, 2162, 1663, 1580, 1492, 1387, 1236, 1089, 1065, 1028, 968, 701 cm^{-1}; Powder X-ray Analysis (I/I_0) 14.13 Å (1.00), 7.06 Å (0.15), 4.75 Å (0.04), 4.04 Å (0.13), 3.54 Å (0.14). Anal. Calcd for $C_{34}H_{40}N_4O_7$: C, 66.21; H, 6.54; N, 9.08. Found: C, 66.16; H, 6.50; N, 9.16.

*Anhydrous (R,R)-**1**·(R)-**2**:* colorless plate crystals: mp 158.2°C dec.; ^{1}H NMR (300 MHz: D_2O) δ 1.62 (d, J=6.9 Hz, 6H), 4.48 (q, J=6.9 Hz, 2H), 5.14 (s, 2H), 7.34–7.51(m, 20H); IR (KBr): 3373, 3036, 2978, 2937, 2170, 1676, 1577, 1476, 1386, 1234, 1188, 1066, 742, 697 cm^{-1}; Powder X-ray Analysis (I/I_0) 11.92 Å (0.67), 11.34 Å (0.29), 10.10 Å (1.00), 6.82 Å (0.23), 5.97 Å (0.24), 5.85 Å (0.65), 5.75 Å (0.24), 5.15 Å (0.77), 5.04 Å (0.23), 4.86 Å (0.59), 4.42 Å (0.56), 4.31 Å (0.44), 4.00 Å (0.46), 3.94 Å (0.73), 3.58 Å (0.36), 3.41 Å (0.34), 3.34 Å (0.28), 2.80 Å (0.17). Anal. Calcd for $C_{34}H_{38}N_4O_6$: C, 68.21; H, 6.40; N, 9.36. Found: C, 68.09; H, 6.49; N, 9.31.

*(R,R)-**1**·(S)-**2**:* colorless plate crystals: mp 180°C dec.; ^{1}H NMR (300 MHz: D_2O) δ 1.64 (d, J=6.9 Hz, 6H), 4.54 (d, J=6.9 Hz, 2H), 5.16 (s, 2H), 7.35–7.51 (m, 20H); IR (KBr): 3341, 3060, 3036, 2968, 2924, 2190, 1663, 1578, 1492, 1396, 1375, 1234, 1092, 1064, 770, 695 cm^{-1}; Powder X-ray Analysis (I/I_0) 13.50 Å (0.56), 6.74 Å (1.00), 4.47 Å (0.08), 3.36 Å (0.38). Anal. Calcd for $C_{34}H_{38}N_4O_6$: C, 68.21; H, 6.40; N, 9.36. Found: C, 68.26; H, 6.29; N, 9.31.

*meso-**1**·(±)-**2**:* colorless plate crystals: mp 180°C dec.; ^{1}H

NMR (300 MHz: D_2O) δ 1.63 (d, J=7.0 Hz, 6H), 4.52 (d, J=7.0 Hz, 2H), 5.18 (s, 2H), 7.30–7.51 (m, 20H); IR (KBr): 3347, 3062, 3036, 2936, 2150, 1659, 1491, 1387, 1238, 1186, 1092, 1064, 758, 728, 699 cm^{-1}; Powder X-ray Analysis (I/I_0) 15.49 Å (1.00), 7.70 Å (0.04), 5.12 Å (0.03), 3.84 Å (0.17).3.07 Å (0.03). Anal. Calcd for $C_{34}H_{38}N_4O_6$: C, 68.21; H, 6.40; N, 9.36. Found: C, 67.93; H, 6.26; N, 9.27.

*meso-**1**·(R)-**2**:* colorless plate crystals: mp 189.2°C dec.; ^1H NMR (300 MHz: d^4-CD_3OD) δ 1.57 (d, J=6.9 Hz, 6H), 4.37 (q, J=6.9 Hz, 2H), 5.16 (s, 2H), 7.20–7.45 (m, 20H); IR (KBr): 3344, 3031, 2925, 2132, 1658, 1592, 1494, 1384, 1240, 1198, 1093, 1066, 730, 698 cm^{-1}; Powder X-ray Analysis (I/I_0) 14.97 Å (1.00), 7.52 Å (0.05), 5.02 Å (0.05), 3.77 Å (0.17). Anal. Calcd for $C_{34}H_{38}N_4O_6$: C, 68.21; H, 6.40; N, 9.36. Found: C, 67.88; H, 6.35; N, 9.27.

Acknowledgements

This work was supported by Grant-in-Aids for Research for the Future Program (JSPS-RFTF96P00304) and Encouragement of Young Scientists (No. 11750733) from the Japan Society for the Promotion of Science.

References

1. Solid-state Supramolecular Chemistry: Two- and three-dimensional Inorganic Networks. In *Comprehensive supramolecular chemistry*; Alberti, G.; Bein, T., Eds.; Vol. 7, Oxford: Pergamon Press, 1996.

2. (a) Aakeröy, C. B. *Acta Cryst.* **1997**, *B53*, 569. (b) Desiraju, G. R. *Crystal Engineering: The Design of Organic Solids*; Elsevier: Amsterdam, 1989.

3. (a) Biradha, K.; Dennis, D.; MacKinnon, V. A.; Sharma, C. V. K.; Zaworotko, M. J. *J. Am. Chem. Soc.* **1998**, *120*, 11894. (b) Sharma, C. V. K.; Bauer, C. B.; Rogers, R. D.; Zaworotko, M. J. *Chem. Commun.* **1997**, 1559.

4. (a) Evans, C. C.; Sukarto, L.; Ward, M. D. *J. Am. Chem. Soc.* **1999**, *121*, 320. (b) Russell, V. A.; Etter, M. C.; Ward, M. D. *J. Am. Chem. Soc.* **1994**, *116*, 1941.

5. Lewis, F. D.; Yang, J. S.; Stern, C. L. *J. Am. Chem. Soc.* **1996**, *118*, 12 029.

6. Aakeröy, C. B.; Nieuwenhuyzen, M. *J. Am. Chem. Soc.* **1994**, *116*, 10 983.

7. (a) Coe, S.; Kane, J. J.; Nguyen, T. L.; Toledo, L. M.; Wininger, E.; Fowler, F. W.; Lauher, J. W. *J. Am. Chem. Soc.* **1997**, *119*, 86. (b) Chang, Y.-L.; West, M.-A.; Fowler, F. W.; Lauher, J. W. *J. Am. Chem. Soc.* **1993**, *115*, 5991. (c) Zhao, X.; Chang, Y.-L.; Fowler, F. W.; Lauher, J. W. *J. Am. Chem. Soc.* **1990**, *112*, 6627.

8. (a) Karle, I. L.; Ranganathan, D.; Sha, K.; Vaish, N. K. *Int. J. Peptide Protein Res.* **1994**, *43*, 160. (b) Karle, I. L.; Ranganathan, D. *Int. J. Peptide Protein Res.* **1995**, *46*, 18. (c) Karle, I. L.; Ranganathan, D. *Biopolymers* **1995**, *36*, 323.

9. For a preliminary accounts of this work, see: Akazome, M.; Takahashi, T.; Ogura, K. *Tetrahedron Lett.* **1998**, *39*, 4839.

10. Sada, K.; Maeda, T.; Miyata, M. *Chem. Lett.* **1996**, 837.

11. Brianso, P. M. C. *Acta Cryst.* **1984**, *B32*, 3040.

12. (a) Kinbara, K.; Sakai, K.; Hashimoto, Y.; Nohira, H.; Saigo, K. *J. Chem. Soc., Perkin Trans. 2* **1996**, 2615. (b) de Diego, H. L. *Acta Chem. Scand.* **1994**, *48*, 306. (c) Zingg, S. P.; Arnett, E. M.; McPhail, A. T.; Brthner-By, A. A.; Gilkerson, W. R. *J. Am. Chem. Soc.* **1988**, *110*, 1565. (d) Brianso, P. M.-C.; Leclercq, M.; Jacques, J. *Acta Cryst.* **1979**, *B35*, 2751.

13. The conformations of oxalyl groups in oxalylamide and *N*,*N*′-dimethyloxamide are complete transoid. (a) Ayerst, E. M.; Duke, J. R. C. *Acta Crystallogr.* **1954**, *7*, 588. (b) Adiwidjaja, G.; Voß, J. *Chem. Ber.* **1977**, *110*, 1159.

14. Hydrogen bonding of 12-membered ring structure in several ammonium carboxylates. For recent papers; (a) Kinbara, K.; Hashimoto, Y.; Sukegawa, M.; Nohira, H.; Saigo, K. *J. Am. Chem. Soc.* **1996**, *118*, 3441. (b) Kozma, D.; Böcskei, Z.; Simon, K.; Fogassy, E. *J. Chem. Soc., Perkin Trans. 2* **1994**, 1883.

15. Jorgensen, W. L.; Severance, D. L. *J. Am Chem. Soc.* **1990**, *112*, 4768 (and references therein).

16. (a) Aakeröy, C. B.; Hitchcock, P. B. *J. Mater. Chem.* **1993**, *3*, 1129. (b) Kroon, J.; Duisenberg, A. J. M.; Peerdeman, A. F. *Acta Cryst.* **1984**, *C40*, 645. (c) Molins, E.; Miravitlles, C.; López-Calahorra, F.; Castells, J.; Raventós, J. *Acta Cryst.* **1989**, *C45*, 104.

17. Altomare, A.; Cascarano, G.; Giacovazzo, C.; Guagliardi, A.; Burla, M. C.; Polidori, G.; Camalli, M. *J. Appl. Cryst.* **1994**, *27*, 435.

18. Cambridge Crystallographic Data Centre, 12 Union Road, Cambridge CB2 1EZ, England.

19. Zervas, L.; Winitz, M.; Greenstein, J. P. *J. Org. Chem.* **1957**, *22*, 1515.

20. Brunner, M.; Huber, W. *Helv. Chim. Acta.* **1953**, *36*, 1109.